Metamagnetic Quantum Criticality in $Sr_3Ru_2O_7$

A. J. Schofield[1], A. J. Millis[2], S. A. Grigera[3], and G. G. Lonzarich[4]

[1] School of Physics and Astronomy, University of Birmingham, Edgbaston, Birmingham, B15 2AD, United Kingdom.
[2] Department of Physics, Columbia University, 538 W 120th St, New York, NY 10027 USA.
[3] School of Physics and Astronomy, University of St. Andrews, North Haugh, St Andrews, Fife, KY16 9SS, United Kingdom.
[4] Cavendish Laboratory, Madingley Road, Cambridge, CB3 0HE, United Kingdom.

Abstract. We consider the metamagnetic transition in the bilayer ruthenate, $Sr_3Ru_2O_7$, and use this to motivate a renormalization group treatment of a zero-temperature quantum-critical end-point. We summarize the results of mean field theory and give a pedagogical derivation of the renormalization-group equations. These are then solved to yield numerical results for the susceptibility, the specific heat and the resistivity exponent which can be compared with measured data on $Sr_3Ru_2O_7$ to provide a powerful test for the standard framework of metallic quantum criticality. The observed approach to the critical point is well-described by our theory explaining a number of unusual features of experimental data. The puzzling behaviour very near to the critical point itself, though, is not accounted for by this, or any other theory with a Fermi surface.

1 Introduction

The presently interesting ruthenium-oxide metals provide a useful test-bed for basic theoretical ideas in the strongly correlated electron problem. The single-layer ruthenate Sr_2RuO_4, being isostructural and isoelectronic with the parent compound of a cuprate superconductor, La_2CuO_4, was original studied as an example of a conventional quasi-2D Fermi-liquid metal [20] against which to compare the more exotic cuprates. The discovery [21] of what now appears to be triplet superconductivity [28] shows that this compound is fascinating in its own right as well as providing a new perspective on cuprate physics. In this paper we discuss the bilayer version of this compound, $Sr_3Ru_2O_7$, and argue that the metamagnetism in this material [27,14] provides an important test for the conventional framework [17,23] of quantum-critical points in metals.

A metamagnetic transition is empirically defined as a rapid increase in magnetization at a particular value of applied magnetic field. Because there is no broken symmetry involved, one expects a first-order transition from a low-magnetization to a high-magnetization state as an applied magnetic field, H, is swept through a (temperature-dependent) critical value, $H_{\rm mm}(T)$. Near a first order transition, kinetics may be complicated but thermodynamic fluctuation corrections to observables should not be divergent or particularly large. However in general, the curve of first-order transitions, $H_{\rm mm}(T)$, terminates in a second-order critical point (H^*, T^*) which is characterized by divergent fluctuations [see Fig. 1(a)]. Furthermore, by appropriately tuning material parameters

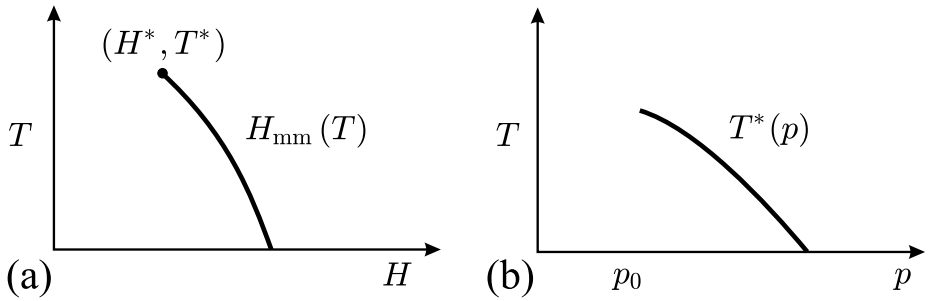

Fig. 1. (a) Schematic phase diagram in the H, T plane showing a line of first-order metamagnetic transitions terminating in a critical end-point. (b) This critical end-point can by suppressed to lower temperatures using a suitable tuning parameter (such as pressure). At a critical pressure, p_0, we have pushed the end-point to $T = 0$ giving the quantum critical end-point discussed in this paper.

(by applying pressure for example) it should be possible to reduce T^* to zero temperature, yielding a *quantum-critical end-point*. This situation is illustrated in Fig. 1 (b) which shows a possible variation of the temperature of the critical end-point with pressure. At a critical end-point there are important fluctuation effects and near a quantum critical end-point the quantal nature of these fluctuations also needs to be taken into account.

The bilayer ruthenate is not unique in showing metamagnetism. A number of 'strongly correlated metals', including UPt_3 [34], $CeRu_2Si_2$ [15,2,12], $CeRh_2Si_2$ [16] and other heavy fermion compounds [1], as well as d-electron systems such as MnSi [35] exhibit metamagnetic transitions with properties suggestive of proximity to a quantum critical point. What makes $Sr_3Ru_2O_7$ [27] stand out is that at ambient pressure and moderate applied field it seems that this material is tuned almost exactly to such a quantum-critical end-point [14]. By a direct comparison of our theory with experiments we show that this system is indeed close to a quantum-critical end-point. In addition, we are able to explain a number of heretofore puzzling features observed in this system: the finite temperature peak in the weak-field susceptibility [18] and the paramagnetic ground state in a metal that should, according to band-structure calculations, be ferromagnetic [32].

Quantum critical transitions in itinerant electron systems have themselves also attracted widespread interest. Generally they are reached by tuning the ordering temperature of a second order phase transition to absolute zero using a control parameter, such as pressure [19] or chemical composition [36]. The critical fluctuations of the slow mode associated with the ordering often influences a wide region of the temperature/tuning parameter phase diagram. The effect of these fluctuations is the appearance of non-Fermi liquid temperature dependences in quantities such as the resistivity, specific heat and the Pauli susceptibility [23]. Indeed it has been suggested that the proximity to a quantum critical point may be the root cause of much of the non-Fermi liquid seen in nature even when there is no obvious symmetry breaking phase transition in the phase diagram.

One possibility is that the order is present but hidden [9]. Alternatively, the quantum critical point is argued to be close to the physical system in the sense that one could tune to it but only through the application of some unphysical tuning parameter (such as negative pressure), though the physical system is affected by the "almost critical" modes of this transition [13]. In this paper we investigate a third possibility: a quantum critical end-point.

An appealing feature of quantum criticality from a theoretical perspective is that an established and tractable theory has been developed [17,23]. However a number of the experimental realizations of quantum-critical systems show deviations from the predicted behaviour [31] which have caused some to question its validity [11]. Factors omitted in the original theory include other, non-critical, slow modes [4], the possible influence of disorder [29] and the Kondo effect [11]. We shall show that these factors should not be present at a metamagnetic quantum-critical end-point and so the theory we present will provide a clean test of the standard [17,23] framework when compared with experiments.

There have been a number of mean-field treatments of metamagnetism in metals recently [22,30] and some discussion was given in the context of a treatment of weak ferromagnets via the 'SCR' method [37,38]. Our work gives, we believe, the first analysis of the critical phenomena at a metamagnetic point. In this paper we give a pedagogical account of our renormalization group theory of metamagnetic quantum criticality—specializing here to the case of a two dimensional system as is appropriate for the layered ruthenates. A brief account of our results for $Sr_3Ru_2O_7$ and the more general case is shortly to be published [24].

2 Deriving the action

The starting point for the treatment is the standard functional integral approach [26] to the interacting-electron problem where we have assumed that the important interaction is a spin-density interaction. This is then decoupled by introducing a Hubbard-Stratonovich field

$$\mathcal{Z} = \int \mathcal{D}(\bar{\psi},\psi) e^{-\int_0^{\hbar\beta} d\tau \sum_{\mathfrak{q}} \left[\bar{\psi}_{\mathfrak{q}}(\tau)(\partial_\tau + \epsilon_{\mathfrak{q}} - \mu)\psi_{\mathfrak{q}}(\tau) - J(\boldsymbol{q})\boldsymbol{S}_{\mathfrak{q}}(\tau)\cdot\boldsymbol{S}_{-\mathfrak{q}}(\tau)\right]}, \tag{1}$$

$$= \int \mathcal{D}(\bar{\psi},\psi,\boldsymbol{\phi}) \exp\left[- \int_0^{\hbar\beta d\tau} \sum_{\boldsymbol{q},\alpha} \frac{1}{4J(\boldsymbol{q})\lambda^2} \boldsymbol{\phi}_{\boldsymbol{q},\alpha}\boldsymbol{\phi}_{-\boldsymbol{q},\alpha} \right.$$

$$\left. + \int d^D\boldsymbol{r} \bar{\psi}_\alpha(\boldsymbol{r},\tau) \left\{ \delta_{\alpha,\beta}\left(\partial_\tau + \epsilon(-i\hbar\boldsymbol{\nabla}) - \mu\right) + i\lambda\boldsymbol{\phi}(\boldsymbol{r})\cdot\sigma_{\alpha\beta} \right\} \psi_\beta(\boldsymbol{r},\tau) \right] \tag{2}$$

The key assumption lying behind the standard approach developed by Hertz [17] and refined by Millis [23] is that the electronic degrees of freedom may be integrated out leaving a model of an over-damped bosonic modes which may then be analysed by renormalization-group methods. It is this procedure that we follow

here. Doing the integration over the fermion Grassmann fields, ψ, yields

$$\mathcal{Z} = \mathcal{Z}_0 \int \mathcal{D}\phi e^{\left[-\int_0^{\hbar\beta} d\tau \sum_{\mathrm{q},\alpha} \frac{1}{4J(\mathrm{q})\lambda^2} \boldsymbol{\phi}_{\mathrm{q},\alpha}\boldsymbol{\phi}_{-\mathrm{q},\alpha} + \int d^2\boldsymbol{x} \ln\det\{\partial_\tau + \epsilon(-i\hbar\boldsymbol{\nabla}) - \mu + i\lambda\boldsymbol{\phi}\cdot\boldsymbol{\sigma}\}\right]} . \tag{3}$$

This "ln det" term is then expanded in powers of the field to give the effective action. The leading order term contains the important dynamics

$$S_{\mathrm{G}}[\phi] = \frac{1}{2}\sum_{\omega_n,\boldsymbol{q}} \left[\frac{1}{4J(\boldsymbol{q})\lambda^2} + \frac{\lambda^2}{2}\Pi(\boldsymbol{q},\omega)\right] \boldsymbol{\phi}_{-\omega_n,-\boldsymbol{q}} \cdot \boldsymbol{\phi}_{\omega_n,\boldsymbol{q}} \, . \tag{4}$$

Here $\Pi(\boldsymbol{q},\omega_n)$ is the Lindhard function, which comes from the fermion bubble obtained by expanding the determinant. Redefining the fields (using λ) to make them dimensionless and expanding the Lindhard function we obtain the Gaussian action

$$S_{\mathrm{G}}[\phi] = \frac{1}{2}\sum_{\omega_n,\boldsymbol{q}} E \left[r + \xi^2\boldsymbol{q}^2 + \frac{|\omega_n|}{vq}\right] \boldsymbol{\phi}_{-\omega_n,-\boldsymbol{q}} \cdot \boldsymbol{\phi}_{\omega_n,\boldsymbol{q}} \, . \tag{5}$$

Here $\xi \sim 1/k_F$, $v \sim v_F$, E is an electronic energy scale and $r = 1 - J(0)/E$ is a measure of the deviation of the system from the Stoner instability [33]: when the reduction in interaction energy from mean-field ordering more than compensates for the consequential increase in kinetic energy. We have used a conventional gradient expansion for the static part of the action and assumed that the coefficients are simple numbers and that the parameters vary weakly with temperature (as T^2, as usual in Fermi-liquid theory). For an $O(3)$ ferromagnetic quantum critical point this may not be the case [5,10], but in the presence of a symmetry breaking field, the T^2 and gradient expansions are believed [4] to apply.

The frequency dependence above is a consequence of the conservation-laws of the order parameter, ϕ. Since ϕ is essentially the difference in position of the "spin-up" and "spin-down" Fermi surfaces, then fluctuations at nonzero q correspond to locally increasing the number of "spin-up" electrons and decreasing the number of "spin-down" electrons. If "spin" is conserved such a fluctuation can relax only via propagation or diffusion of electrons within each spin manifold. This must vanish as $q \to 0$. Quotes are placed about "spin up" and "spin down" because in many metamagnetic materials spin-orbit coupling is large and spin is not a good quantum number. However, for most purposes one may adopt a 'pseudo-spin' notation [6] labelling the two Kramers-degenerate states in zero-field. The Kramer's degeneracy is broken by an applied field, leading to two Fermi surfaces and the theory carries through as in the non-spin-orbit case: since in a clean spin-orbit-coupled system, pseudo-spin is conserved (at least for fields aligned along a crystal symmetry axis). There is one exception to this—disorder scattering in the presence of strong spin-orbit coupling can allow pseudo-spin relaxation even as $q \to 0$. Then the vq term would be replaced by a momentum independent constant leading to a dynamical exponent of $z = 2$ (see later).

Further expansion in the fields $\boldsymbol{\phi}$ adds interaction terms to the action giving the final form of the action

$$S[\phi] = S_{\mathrm{G}} + \int d^2x d\tau \frac{1}{4} u_{ab}\phi_a^2\phi_b^2 + \frac{1}{6} v_{abc}\phi_a^2\phi_b^2\phi_c^2 - g\mu_B \boldsymbol{H}\cdot\boldsymbol{\phi}(\boldsymbol{x},\tau) + \cdots \, . \tag{6}$$

In writing the action above we have in mind the case of $Sr_3Ru_2O_7$ so are specializing to the case of two dimensions. The subscripts on the fields are components of the vectors and are summed over. Experimentally it is known that at zero temperature the weak-field susceptibility is isotropic which implies no directional dependence of r or g. It becomes anisotropic at finite magnetic field and/or temperature where, as we will see, higher order terms in the expansion become important—hence in general u and v are anisotropic tensors. Obtaining the anisotropy theoretically requires inclusion of spin-orbit effects not explicitly written in Eq. 3 above. We choose units such that the field ϕ is measured relative to the saturation magnetization: $2\mu_B$/Ru. (The important electrons are in d shells with four in t_{2g} which leaves two holes and the g factor should be close to 2.)

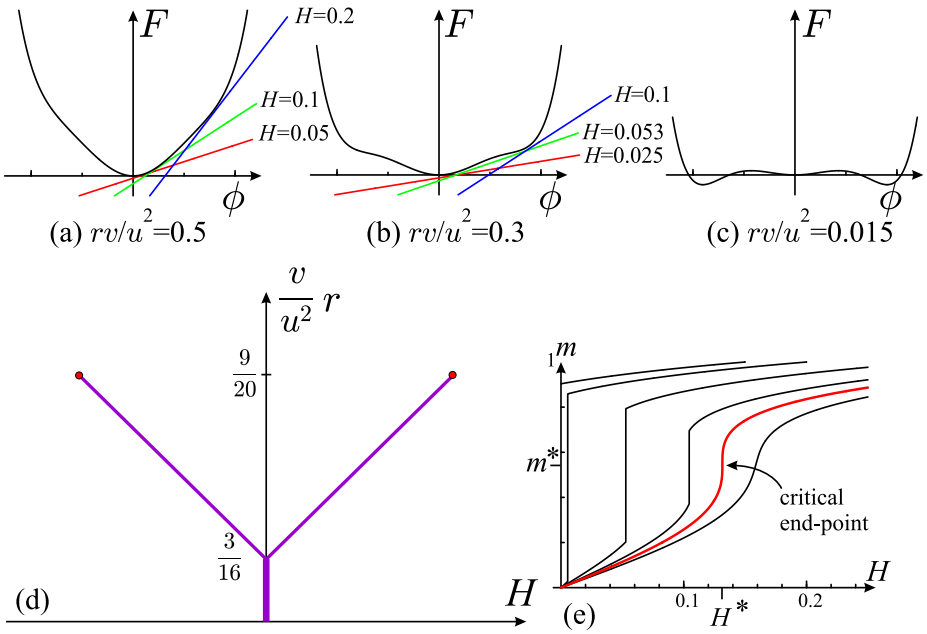

Fig. 2. Mean field treatment of the magnetization from Eq. 7. The phase diagram depends on rv/u^2 and the equilibrium magnetization is found when the tangent to the free energy curves equals the magnetic field (here measured in units of $g\mu_B$). This is illustrated in (a) to (c). The general phase diagram is shown in (d) where the lines represent the metamagnetic transition for $9/20 < rv/u^2 < 3/16$. For $rv/u^2 > 9/20$ we have crossover behaviour and no transition. For $rv/u^2 < 3/16$ the system is unstable to a first order ferromagnetism even in the absence of an applied field. The critical end-point of the metamagnetism occurs at $rv/u^2 = 9/20$ where the magnetization has infinite slope at the critical field as show in (e).

3 Mean-field theory

To develop an understanding of this model we consider it first in mean-field theory ignoring the effect of fluctuations, both quantal and spatial, by suppressing the τ, ω and $\boldsymbol{x}, \boldsymbol{q}$ dependence and treating the action as a free energy:

$$F[\phi] = \frac{1}{2} r\phi^2 + \frac{1}{4} u\phi^4 + \frac{1}{6} v\phi^6 + g\mu_B H\phi \, . \tag{7}$$

We have suppressed the vector nature of the field ϕ for simplicity here. To obtain a metamagnetic transition we require that $r > 0$ so that the ground state is paramagnetic, but that the fourth order term u is negative ($v > 0$ controls the expansion). The equilibrium magnetization, $\bar{\phi}$, is then found by minimizing the action. The solutions are when the tangent to the free energy, $\partial F/\partial\phi$, is equal to $g\mu_B H$. Such solutions are shown graphically in Fig. 2(a)–(c). The form of the phase diagram is shown in Fig.2 where it can be seen that the ratio rv/u^2 determines the transitions. For $9/20 < rv/u^2 < 3/16$ we have a first order metamagnetic transition signalled by a jump in the magnetization at finite magnetic field [see Fig. 2(e)]. The critical end-point of the metamagnetic transitions occurs when $F[\phi]$ first develops an inflection point: at $rv/u^2 = 9/20$. The magnetization then has infinite slope at a critical field, H^*. At the critical end-point and for fields in the c-direction (restoring the tensorial nature of the terms)

$$m_c^* = \sqrt{\frac{-3u_{cc}}{10v_{ccc}}} \, , \qquad g_{\rm eff}\mu_{\rm B} H_c^* = \sqrt{\frac{-3u_{cc}}{10v_{ccc}}} \frac{6u_{cc}^2}{25v_{ccc}} \, . \tag{8}$$

Comparison with experimental data on $Sr_3Ru_2O_7$ allows us to fix parameters for the theory. Fig. 1 of Ref. [27] shows that at low T and low applied field the susceptibility is about $0.025\mu_{\rm B}/T$ implying $r \approx 160\mu_{\rm B} - T \approx 100$K. This small value of r implies a very large enhancement of the susceptibility, $\chi \approx 1/r$, over the band value—the material is near a paramagnetic-ferromagnetic transition. For fields directed along the c axis the observed metamagnetic transition occurs at a magnetization of about $0.25 - 0.3\mu_{\rm B}$/Ru implying $u_{cc} = 3000 - 4300$K and $v_{ccc} = 40,000 - 80,000$K with the larger values corresponding to the smaller m. The consistency of these estimates may be verified by substitution into Eq. 8; use of $g_{\rm eff} = 2$ yields an estimate of $5 - 6$T for the metamagnetic field, in the range found experimentally. The scale E is of order 6000K-8000K. The dimensionless critical field $g\mu_B H^*/u \sim 0.001$. If we are concerned with the behaviour in the vicinity of the critical end-point then we should look at small deviations with respect to this already small value. At present rather less information about the spin fluctuation frequencies is available [8]. Therefore when comparing the results of our renormalization group analysis with experiment, we will normalize our results results to the temperature T_0 at which the differential susceptibility at the critical field is equal to the zero-field zero temperature susceptibility, *i.e* $\frac{\partial m}{\partial h}(\delta = 0, T = T_0) = \chi(H = 0, T = 0) = \chi_0$.

4 Tree-Level Scaling

Having considered the model at mean field, we now proceed to treat the full quantum action of Eq. 6 via the renormalization group. The method we are using is that of Ref. [23] and for completeness we outline the steps involved. The first step is to perform "tree-level scaling" of the parameters in the action, which follows from a dimensional analysis. This only involves power-counting so we write the action to emphasize this

$$S = H\cdot\phi + \int^{\Lambda} d^2k d\omega \left[r + \xi^2 k^2 + \frac{|\omega_n|}{vk} \right] \phi^2 + u \int^{\Lambda} (d^2k d\omega)^3 \phi^4 + v \int^{\Lambda} (d^2k d\omega)^5 \phi^6 + \cdots . \tag{9}$$

Now the idea is to let the momentum bandwidth be rescaled: $\Lambda(\lambda) = \Lambda e^{-\lambda}$. Then all the coupling constants and fields will be rescaled to preserve the same physics and so become functions of λ. Writing $b = e^{\lambda}$ we have $\Lambda \to \Lambda/b$. To restore the momentum cutoff we must have $\tilde{k} = bk$. Now this forces the gradient term (proportional to k^2) to have an extra factor of $1/b^2$ so to maintain the same form of the Gaussian part of the action we need to be able to pull out a b^{-2} factor from every term. This dictates the scaling of r and ω. So, $r = \tilde{r}/b^2$ and hence we have

$$r(\lambda) = re^{2\lambda} \qquad \Leftrightarrow \qquad \frac{\partial r}{\partial \lambda} = 2r \; . \tag{10}$$

Also $\omega/k \to \tilde{\omega}/(b^2\tilde{k})$ so this means that $\omega = \tilde{\omega}/b^3 \to [\omega] = 3$. This is the dynamical exponent and is often denoted z. We then absorb all of the b factors into a rescaling of the field ϕ. There are two sources, the Jacobians from the change of variables which will generate b^{-5}, and the $1/b^2$ factor from the coefficient of the Gaussian term. Thus we have an overall factor of b^{-7}. To absorb this, the field ϕ must scale as $\tilde{\phi} = b^{-7/2}\phi$. This, in turn, dictates the scaling of the magnetic field: $\tilde{h} = b^{+7/2}h$. It also then fixes the form of the u and v part of the action. In the ϕ^4 term we have 3 powers of phase space integrals and 4 powers of the field giving b^{-1} which must be absorbed by a renormalization of u : $\tilde{u} = b^{-1}u$. In the ϕ^6 term we have 5 powers of phase space integrals and 6 powers of the field giving b^{-4} which must be absorbed by a renormalization of v : $\tilde{v} = b^{-4}v$. Thus writing, $\lambda = \ln b$, we have the following scaling equations at tree level:

$$\frac{\partial r}{\partial \lambda} = 2r \; , \tag{11}$$

$$\frac{\partial h}{\partial \lambda} = \frac{7}{2}h \; , \tag{12}$$

$$\frac{\partial u}{\partial \lambda} = -u \; , \tag{13}$$

$$\frac{\partial v}{\partial \lambda} = -4v \; . \tag{14}$$

The remaining scaling equation is for the temperature. This is not so obvious perhaps from the above analysis. However, if we consider any physical quantity

calculated in the theory then the scaling of temperature becomes apparent. We will use the free energy computed from the Gaussian part of the action. The free energy is found from the partition function, $\beta F = -\ln Z$. Now working to Gaussian order only we find

$$\begin{aligned} Z &= Z_0 \int \mathcal{D}\phi \exp\left[-S_{\rm G}(\phi)\right] \\ &= Z_0 \prod_{n,\boldsymbol{k}} \frac{1}{r + \xi^2 k^2 + |\omega_n|/\Gamma_k} \,, \end{aligned} \tag{15}$$

$$\text{So} \quad F = F_0 + \frac{V}{\beta} \int \frac{d^2k}{(2\pi)^2} \sum_n \ln\left[r + \xi^2 k^2 + |\omega_n|/\Gamma_k\right] \,. \tag{16}$$

where $\Gamma_k = vk$ is the Landau damping rate.

Handling Matsubara sums involving $|\omega_n|$ will recur in this paper so we give some of the details here of how these are treated. The Matsubara sum is over $\omega_n = 2\pi n/\beta$ and is formally divergent. We can regularize it by considering $\oint \frac{dz}{2\pi i} n_B(z) f(z)$, where $f(z)$ is the function we wish to sum over Matsubara frequencies (here the logarithm) and n_B is the Bose distribution. The contour of integration is taken as a large radius circle centred on the origin. This contour integral is divergent just as the sum is, however its divergence is temperature independent as the contour is taken to infinity and so can be subtracted. Thus we essentially do the Matsubara sum using the usual contour integral technique as if it did converge and the contour integral was zero.

Now $n_B(z)$ has poles of residue $1/\beta$ at the Matsubara frequencies so the sum over its residues will give the required Matsubara sum. The analytic structure of the logarithm requires knowing, in term, the analytic structure of $|\omega_n|$. This comes from its origin in the Lindhard function where we find that

$$\frac{z}{\pi\Gamma} \ln\left(\frac{z+\Gamma}{z-\Gamma}\right) \to \frac{|\omega|}{\Gamma} \quad \text{for } z \to i\omega \,. \tag{17}$$

Thus $f(z)$ has a branch cut along the real axis between $-\Gamma$ and Γ. Finally the Matsubara sum plus the integral around the branch-cut must combine to give the value of the large radius contour integral (which we take to be zero as detailed above). This allows us to evaluate the sum. (There is a pole on the branch-cut but this will be taken care of by the principle part of the line integral.) So we have, for each mode k (and using $\eta = r + \xi^2 k^2$),

$$F = \frac{1}{\beta} \sum_n \ln\left(\eta + |\omega_n|/\Gamma\right) \,, \tag{18}$$

$$= -\int_{-\Gamma}^{\Gamma} \frac{d\omega}{2\pi i} n_B(\omega) \ln(\eta - i\omega/\Gamma) + \int_{-\Gamma}^{\Gamma} \frac{d\omega}{2\pi i} n_B(\omega) \ln(\eta + i\omega/\Gamma) \,, \tag{19}$$

$$= -\int_{-\Gamma}^{\Gamma} \frac{d\omega}{2\pi} n_B(\omega) 2\tan^{-1}\left(\frac{\omega}{\eta\Gamma}\right) \,. \tag{20}$$

This can be viewed as the definition of the free energy of an overdamped simple harmonic oscillator—so confirming our regularization procedure. Now note that we can write the Bose factor in terms of an odd and an even function

$$n_B(\omega) = \frac{1}{2}\left(\coth\left[\frac{\omega}{2k_BT}\right] - 1\right) . \tag{21}$$

Since the other term in the free energy is odd then we only need the odd part of Bose factor and we can halve the integration range, thereby giving for each mode

$$F = -\int_0^\Gamma \frac{d\omega}{\pi}\coth\left(\frac{\omega}{2k_BT}\right)\tan^{-1}\left(\frac{\omega}{\eta\Gamma}\right) . \tag{22}$$

Thus our full expression for the free energy (per unit volume) is

$$F = -\int^\Lambda \frac{d^2k}{(2\pi)^2}\int_0^{\Gamma_k}\frac{d\omega}{\pi}\coth\left(\frac{\omega}{2k_BT}\right)\tan^{-1}\left(\frac{\omega/\Gamma_k}{r+\xi^2k^2}\right) . \tag{23}$$

Now we imagine reducing the momentum cutoff as before: $\Lambda \to \Lambda/b$ where $b \sim 1+\epsilon$, and then perform the rescaling to restore, this time, the form of the equation for the free energy to the original one (Eq. 23). Just as before, we must have $\tilde{k} = kb$. Then in order for the argument of $\tan^{-1}$ to be preserved, we must have $\tilde{r} = b^2 r$ and $\tilde{\omega} = b^3\omega$. This now forces the scaling of T from the argument of the coth such that $\tilde{T} = b^3 T$. So we have the RG equation for T

$$\frac{\partial T}{\partial \lambda} = 3T . \tag{24}$$

The rescaling of ω implies that to restore the form of the equation for the free energy, we need to change the frequency cutoff to $\Gamma_{\tilde{k}}$. So as well as removing high momentum modes the rescaling means that we are losing some high frequency modes at *all* momenta. The effect of rescaling on the cutoffs is illustrated in Fig. 3, where the shaded region shows the modes that are being removed.

5 One-Loop Corrections

We now consider the one-loop corrections to the scaling equations to lowest order. The modes above the cutoff (as shaded in Fig. 3) are denoted $>$ while the remaining modes are superscripted as $<$. We perturbatively include the effects of the modes above the cutoff by renormalizing terms in the effective action of the remaining $<$ sector:

$$\mathcal{Z} = \int \mathcal{D}[\phi^<]\mathcal{D}[\phi^>]e^{-S_{\rm G}[\phi^<]-S_{\rm G}[\phi^>]-S_{\rm I}[\phi^<,\phi^>]} , \tag{25}$$

$$= \int \mathcal{D}[\phi^<]\mathcal{D}[\phi^>]e^{-S_{\rm G}[\phi^<]-S_{\rm G}[\phi^>]}\left(1 - S_{\rm I}[\phi^<,\phi^>] + \cdots\right) , \tag{26}$$

$$= \int \mathcal{D}[\phi^<]e^{-S_{\rm G}[\phi^<]}\left(1 - \langle S_{\rm I}[\phi^<,\phi^>]\rangle_>[\phi^<] + \cdots\right) , \tag{27}$$

$$= \int \mathcal{D}[\phi^<]e^{-S_{\rm G}[\phi^<]-\langle S_{\rm I}[\phi^<,\phi^>]\rangle_>[\phi^<]+\cdots} . \tag{28}$$

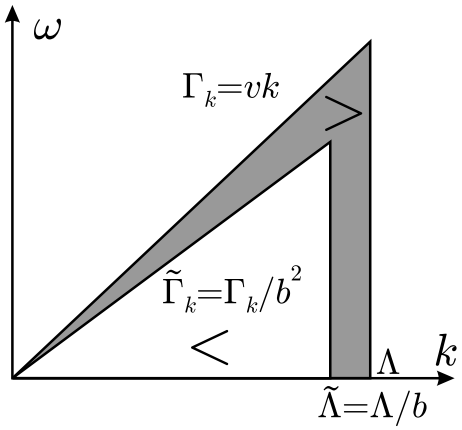

Fig. 3. When rescaling the k cutoff from Λ to $\tilde{\Lambda} = \Lambda/b$ preserving the form at a Gaussian level requires that the frequency cutoff is also rescaled: Γ_k becomes $\tilde{\Gamma}_k = \Gamma_k/b^2$. The rescaling is independent of dynamical exponent z. The modes which are lost by this process are shaded.

Thus we obtain, perturbatively, a low energy effective action where the average is taken by integrating out the regions above the cut-off.

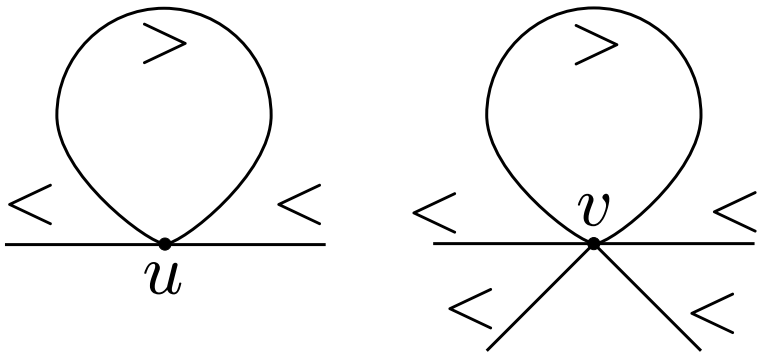

Fig. 4. The 1 loop contribution to the RG equations which renormalize r and u. The loop is summed over the high momentum and frequency modes $>$ illustrated in Fig. 3

At lowest order in u we would have a correction coming from one loop which renormalizes r as shown in Fig. 4. It produces an identical term to that renormalizing u from v except for a combinatorial factor for an n component field which comes from the number of ways of closing the loop. Doing the combinatorics gives $2n + 4$ for the u-loop and $3n + 12$ for the v-loop.

Now in evaluating the diagrams of Fig. 4 we must integrate over the eliminated modes within the Gaussian approximation. (Strictly this is the Gaussian

approximation for fluctuations of the field *about the equilibrium value* as discussed later [Eq. 51] so we should replace the zero-field inverse-susceptibility, r, by the differential value at the field where scaling is being done, δ. Ultimately though the modes we are integrating over are at the cut-off scale so we will be able to set this mass to zero and the distinction is not important.) The diagram as a whole (integrating over all modes) would in general have the following form:

$$f_{\rm all} = \int_0^\Lambda \frac{d^2k}{(2\pi)^2} \frac{1}{\beta} \sum_n \frac{1}{r + \xi^2 k^2 + |\omega_n|/\Gamma_k} \ . \tag{29}$$

We do the frequency sum in exactly the same way as we calculated the free energy giving

$$f_{\rm all} = \int_0^\Lambda \frac{d^2k}{(2\pi)^2} \int_0^{\Gamma_k} \frac{d\omega}{\pi} \coth\left(\frac{\omega}{2k_BT}\right) \frac{\omega/\Gamma_k}{(r+\xi^2k^2)^2 + (\omega/\Gamma_k)^2} \ , \tag{30}$$

$$= A \int_0^\Lambda k dk \int_0^{\Gamma_k} d\omega \coth\left(\frac{\omega}{2k_BT}\right) \frac{\omega/\Gamma_k}{(r+\xi^2k^2)^2 + (\omega/\Gamma_k)^2} \ . \tag{31}$$

where $A = \frac{1}{2\pi^2}$. However, for the RG equations we only need this function summed over the missing modes. This can be done in two parts: the momenta between Λ/b and Λ and the frequencies between Γ_k/b^2 and Γ_k.

Considering the high k modes first. The integral over k then becomes trivial since the limits are coalescing. Thus we can replace k by Λ and multiply by the width of the integration region, $\Lambda - \Lambda/b$. Using the fact that for small deviations of b from 1, we may write $1 - b^{-a} \sim a \ln b$ we can write

$$f_k = A\Lambda^2(1-b^{-1}) \int_0^{\Gamma_\Lambda} d\omega \coth\left(\frac{\omega}{2k_BT}\right) \frac{\omega/\Gamma_\Lambda}{(r+\xi^2\Lambda^2)^2 + (\omega/\Gamma_\Lambda)^2} \ , \tag{32}$$

$$= A\Lambda^2 \ln b \int_0^{v\Lambda} d\omega \coth\left(\frac{\omega}{2k_BT}\right) \frac{\omega/v\Lambda}{(r+\xi^2\Lambda^2)^2 + (\omega/v\Lambda)^2} \ . \tag{33}$$

Now putting $x = w/v\Lambda$ we may rewrite the integral as

$$f_k = A \ln b \, v\Lambda^3 \int_0^1 dx \coth\left[\frac{v\Lambda x}{2k_BT}\right] \frac{x}{(r+\xi^2\Lambda^2)^2 + x^2} \ . \tag{34}$$

Now we do the same for the high ω modes. For each k I have a trivial ω integral to do with the limits coalescing: $\Gamma_k/b^2 < \omega < \Gamma_k$. Thus we have

$$f_\omega = A \int_0^\Lambda k \, dk \Gamma_k (1-b^{-2}) \coth\left(\frac{\Gamma_k}{2k_BT}\right) \frac{1}{(r+\xi^2k^2)^2 + (1)^2} \ , \tag{35}$$

$$= 2A \ln b \int_0^\Lambda dk \, k^2 v \coth\left[\frac{vk}{2k_BT}\right] \frac{1}{(r+\xi^2k^2)^2 + 1} \ . \tag{36}$$

Now putting $y = k/\Lambda$ we may rewrite this terms as

$$f_\omega = 2A \ln b \, v\Lambda^3 \int_0^1 dy \coth\left[\frac{v\Lambda y}{2k_BT}\right] \frac{y^2}{(r+\xi^2\Lambda^2y^2)^2 + 1} \ . \tag{37}$$

Now we can identify the energy scales in the problem. One recurring scale is

$$v_F \Lambda = \Gamma_\Lambda = \omega_{\rm sf} \ , \tag{38}$$

which is the damping rate of spin-fluctuations at the cut-off.

Finally, as noted above, we can set $r = 0$ since the $>$-sector modes are far from the criticality, so defining the following function (where $t = k_B T/\omega_{\rm sf}$ and setting $\xi\Lambda = 1$)

$$f(t) = A \int_0^1 du \coth\left(\frac{u}{2t}\right) \left[\frac{u}{u^2+1} + 2\frac{u^2}{u^4+1}\right] \ . \tag{39}$$

Thus at 1-loop the RG equations become modified ($\lambda = \ln b$) so that

$$\frac{dr}{d\lambda} = 2r + \frac{n+2}{2} u(\lambda)\, f(t) \ , \tag{40}$$

$$\frac{du}{d\lambda} = -u + \frac{n+4}{2} v(\lambda)\, f(t) \ . \tag{41}$$

6 Integrating the RG equations

To use these scaling equations (Eqs. 12, 14, 24, 40 and 41), together with the definition Eq. 39, we need to solve them. However, the RG equations are simply a set of coupled linear differential equations which may be integrated directly.

Solving the equations for v, T and h is trivial

$$v(\lambda) = v_0 e^{-4\lambda} \ , \qquad t(\lambda) = t_0 e^{3\lambda} \ , \qquad h(\lambda) = h_0 e^{7\lambda/2} \ . \tag{42}$$

We can therefore substitute these results into the equation for u:

$$\frac{du}{d\lambda} - u(\lambda) = \frac{n+4}{2} v_0 e^{-4\lambda} f(t_0 e^{3\lambda}) \ , \tag{43}$$

to be solved subject to the initial condition that $u(0) = u_0$. This again is straightforward

$$u(\lambda) = e^{-\lambda} \left[u_0 + \frac{n+4}{2} v_0 \int_0^\lambda e^{-3x} f(t_0 e^{3x}) dx \right] \ . \tag{44}$$

Now again we can substitute this into the equation for r. Solving this yields

$$\begin{aligned} r(\lambda) &= e^{2\lambda} \left[r_0 + \frac{n+2}{2} \int_0^\lambda dy e^{-2y} f(t_0 e^{3y}) u(y) \right] , \\ &= e^{2\lambda} \left\{ r_0 + \frac{n+2}{2} \int_0^\lambda dy\, e^{-3y} f(t_0 e^{3y}) \left[u_0 + \frac{n+4}{2} v_0 \int_0^y dx\, e^{-3x} f(t_0 e^{3x}) \right] \right\} . \end{aligned} \tag{45}$$

Now we can rewrite the solution of the RG equations into parts which explicitly are temperature dependent, and the remaining $T = 0$ values which are

renormalized from their initial values by quantal fluctuations. Consider the definition of the function $f(t)$ in Eq. 39. We may identify $\coth(y/2t) = 1 + 2n_B(y/t)$ where, for $t = 0$, the Bose factor is zero for all positive y. Thus we may write

$$f(t) = f_0 + g(t) \,, \tag{46}$$

where

$$f_0 \quad = A \int_0^1 du \left[\frac{u}{u^2+1} + 2\frac{u^2}{u^4+1} \right] \sim 0.0422 \,. \tag{47}$$

$$g(t) = A \int_0^1 du\, n_B\left(\frac{u}{t}\right) \left[\frac{u}{u^2+1} + 2\frac{u^2}{u^4+1} \right] \,. \tag{48}$$

The dependence of r and u on f_0 reflects how quantal fluctuations renormalize the bare parameters at $T = 0$ and this can be an appreciable effect (determined by the size of u and v). The sign of these effects is such that they move the system *away* from the magnetically ordered phase. This provides an explanation for the band-structure predictions that $Sr_3Ru_20_7$ should be a ferromagnetic at zero magnetic field [32]: the quantal effects are pushing the metal into the paramagnetic phase.

It is more transparent to write the solution to the scaling equations explicitly in terms of the $T = 0$ renormalized parameters

$$r(\lambda) = e^{2\lambda} \left[r_{\rm eff} + \frac{n+2}{2} \int_0^\lambda dy e^{-3y} \left\{ u_{\rm eff} g(t_0 e^{3y}) + \frac{n+4}{2} v_0 \int_0^y e^{-3x} g(t_0 e^{3x}) dx \right\} \right] . \tag{49}$$

Finally, it is also more convenient for the numerical evaluation to use t as the running variable rather than λ. This then amounts to a change of variables in the equation for r: $t = t_0 e^{3w}$. Thus $dw = dt/(3t)$. Doing this change of variables in each of the integrals we will have

$$r(\lambda) = e^{2\lambda} \left[r_{\rm eff} + \frac{n+2}{2} \int_{t_0}^{t_0 e^{3\lambda}} \frac{dt}{3t} \left(\frac{t_0}{t}\right) \left\{ u_{\rm eff} (3^{-1} \ln t/t_0) g(t) \right.\right.$$
$$\left.\left. + \frac{n+4}{2} v_0 \int_{t_0}^t \left(\frac{t_0}{t'}\right) g(t') \frac{dt'}{3t'} \right\} \right] \,. \tag{50}$$

This is the expression we will use for subsequent numerical evaluation.

7 Numerical Procedure

The process by which we turn the solution of the scaling equations into physical quantities is described as follows (though performed numerically). For a fixed set of initial parameters $r_{\rm eff}$, $u_{\rm eff}$, v_0 and t_0, integrate the RG equations until $r = 1$. This effectively sets the $H = 0$ and $T = 0$ susceptibility to 1 (which is

the normalization for our results). We then use the rescaled parameters at the value of λ which gives $r = 1$.

To analyse the experimental consequences of proximity to metamagnetism we consider Gaussian fluctuations about the equilibrium magnetization as determined from the action now with the renormalized parameters. We expand the field about its equilibrium point: $\varphi = (|\phi| - \bar{\phi})/\phi_0$ normalized to the saturation magnetization (ϕ_0). At the metamagnetic point itself we find $\bar{\phi}^2 = -3u/10v$. We measure the field relative to the critical field $h = (H - H^*)/H^*$. The resulting action at quadratic order looks exactly the same as the Gaussian action for the total magnetization Eq. 5 since its form is determined by symmetry

$$S_{\rm meta} = \int d^2q \sum_n \left[\delta + \xi^2 q^2 + \frac{|\omega_n|}{vq} \right] \varphi_{\boldsymbol{q},\omega_n} \varphi_{-\boldsymbol{q},-\omega_n} \ . \tag{51}$$

However here r has been replaced by δ, the "mass" of the fluctuations, which measures the distance from the quantum critical end-point. Experimentally it is the inverse of the differential susceptibility: $\delta = r + 3u\bar{\phi}^2 + 5v\bar{\phi}^4$. The differential susceptibility, δ^{-1}, diverges at the critical end-point. At the metamagnetic critical end-point ($rv/u^2 = 9/20$) but not quite at the critical magnetic field ($h \neq 0$) then we find, from an expansion of Eq. 7, that

$$\delta = \frac{3r(2\bar{\phi}^2 r^{-1} h)^{2/3}}{\bar{\phi}^2} \ . \tag{52}$$

Analysis of this action alone can be used to determine the qualitative behaviour near the metamagnetic point. The results are reminiscent of a ferromagnetic quantum critical point except that the "mass" is also related to the field h. Results are summarized in Ref. [24]. Note that the detailed temperature dependence of quantities requires integration of the RG equations.

We compute three key quantities: the differential susceptibility, the resistivity exponent and $\gamma = C/T$. The differential susceptibility (δ^{-1}) is obtained directly from the second derivative of the free energy about the equilibrium value (with the rescaled parameters). The linear term in the heat capacity is determined from the second-temperature derivative of the free energy of Eq. 23 but evaluated using the parameters of the Gaussian model of Eq. 51. The resistivity is more involved since we now need to reconsider the electrons which were integrated out. We essentially "undo" the Hubbard Stratonovich of Eq. 2 only now using the Gaussian action for ϕ (Eq. 51 determined using the renormalized parameters). The resistivity then comes from considering the lowest order term in the self-energy that comes from interactions of the electrons with the mode φ. This self-energy must be corrected for the forward scattering physics: the dominant scattering is at long wavelength and so is ineffective at degrading a current.

At lowest order the electron self-energy is

$$\Sigma(\boldsymbol{p}, i\Omega_{n'}) = J^2 \int \frac{d^2q}{(2\pi)^2} \frac{1}{\beta} \sum_n G(\boldsymbol{p} - \boldsymbol{q}, i\Omega_{n'} - i\omega_n) D(\boldsymbol{q}, i\omega_n) \ , \tag{53}$$

where G is the non-interacting electron Green's function and $D(\boldsymbol{q}, i\omega_n) = (\delta + \xi^2 q^2 + |\omega_n|/\Gamma_q)^{-1}$ is the Gaussian propagator of the spin fluctuations. Doing this summation and integral is straightforward particularly since we are interested in the quasiparticle scattering rate at the Fermi surface. For this we need the imaginary part of the self-energy calculated on shell

$$\frac{1}{\tau_{p_F}} = -2\mathrm{Im}\Sigma(\boldsymbol{p}_F, i\Omega_{n'} \to \epsilon_{p_F} + i0^+) \; , \tag{54}$$

and corrected for the $1 - \cos\theta \sim (q/k_F)^2$ forward scattering factor (θ is the scattering angle). After some algebra we find

$$\frac{1}{\tau_{p_F}^{\mathrm{2D}}} \sim \int_0^\infty \frac{qdq}{\pi^2} \left(\frac{q}{k_F}\right)^2 \int_{-v_F}^0 \frac{d\omega'}{v_F q} \frac{1}{\sinh(\omega'\beta)} \frac{2\omega'/\Gamma_q}{(\delta + \xi^2 q^2)^2 + (\omega'/\Gamma_q)^2} \; . \tag{55}$$

8 Results

We have started with an isotropic $n = 3$ vector theory for the magnetization variable (just as would be the case for a ferromagnetic quantum critical point). Refs. [5,3,10] have argued that the spatial gradient structure in this case is dramatically affected by interaction corrections. However in the presence of a magnetic field, the 'mass' (coefficient of the quadratic part of the fluctuations) becomes anisotropic, with the component corresponding to fluctuations along the field becoming $r_{\mathrm{eff}} = r + 3u\overline{\phi}^2 + 5v\overline{\phi}^4$. A Heisenberg-$XY$ or Heisenberg-Ising crossover occurs when then larger of r_{eff} or r passes through unity and scaling stops when the smaller of the two becomes of order unity. Thus in the vicinity of the metamagnetic transition we are only dealing with a one-component, Ising, field as described in Eq. 51 which does not suffer from the deviations mentioned above. Moreover the bilayer ruthenate material is stoichiometric so disorder should not be so important and, being a d metal system, Kondo physics is not relevant. So it seems that none of the possible mechanisms for discrepancies from the conventional theory should apply to the metamagnetic quantum end-point in $Sr_3Ru_2O_7$. Indeed comparison of the theory developed here with experiment provides an excellent test of the theoretical framework.

We now present the results of a numerical solution of the scaling equations. Fig. 5 shows the h dependence of the differential susceptibility for several values of T, obtained in the two dimensional case using parameters reasonable for $Sr_3Ru_2O_7$. The inset shows the temperature dependence of the differential susceptibility for different h. Note the non-monotonic temperature dependence for fields different from $h = 0$ if the control parameter is tuned to criticality. Thus our theory shows that the similar peak seen in the experiments [18] is not an indication of some hidden magnetic order but rather is a natural signature of proximity to a metamagnetic quantum critical end-point.

Fig. 6 shows the specific heat coefficient $\gamma = C/T$; in this quantity the crossover is much less sharp, in part because a 2d nearly critical Fermi liquid has a specific heat coefficient $\gamma \sim A + BT$ with both A and B divergent as the

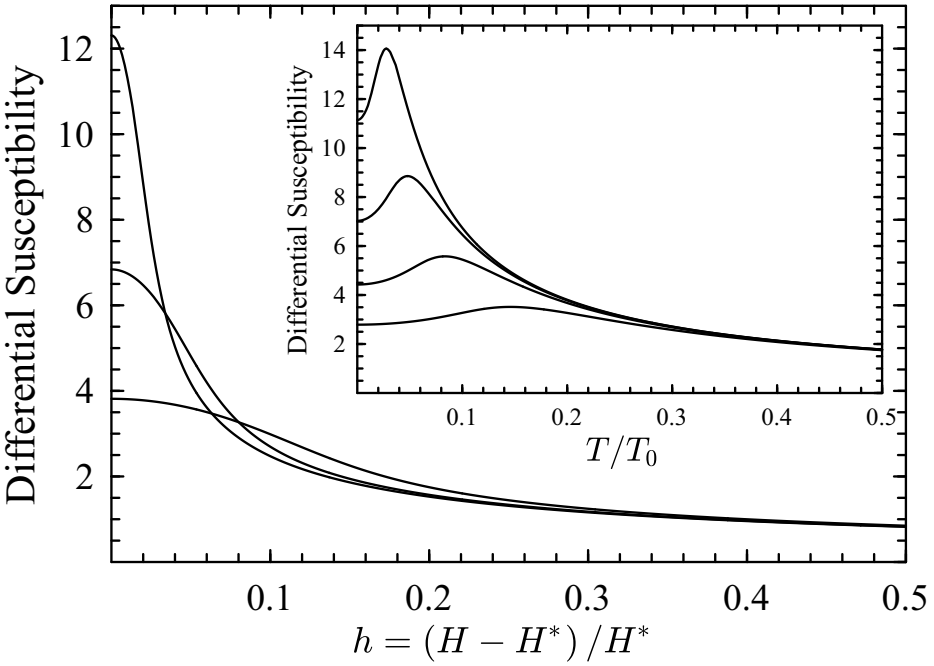

Fig. 5. Differential susceptibility, $\chi_0^{-1}(\partial m/\partial h)$, as a function of applied field H at temperatures $T/T_0 = 0.05, 0.1, 0.2$, for a two dimensional metamagnetic critical point. Inset: Dependence of $\chi_0^{-1}(\partial m/\partial h)$ on temperature T at $h = .01, .02, .04, .08$. (Normalizations discussed in text.)

critical point is approached. This is an example of the corrections to scaling from the one-loop corrections of the irrelevant operators. The inset shows the resistivity exponent $\alpha = -\partial \ln \rho / \partial \ln T$ plotted against temperature for $h = 0$ and $h = 0.1$. The high-T resistivity exponent at a ferromagnetic critical point would naively expected to be 4/3. However the 1-loop corrections modify this value as shown in the inset. The crossover to the expected low-T T^2 behaviour is very sharp. The coefficient of this T^2 resistivity diverges $h^{-2/3}$ as the critical point is approached since it is determined δ (see Eq. 52). This power-law divergence is seen in $Sr_3Ru_2O_7$ as the critical field is approached.

There are, however, two features of the experimental resistivity that this theory cannot explain. The first is that the residual (elastic) part of the resistivity shows a sharp maximum at the critical field. This is presumably a consequence of the interplay between static disorder and the critical fluctuations—which is beyond the scope of this treatment [7]. The second is that at the critical point itself a new temperature dependent resistivity is seen: $\rho \sim \rho_0 + AT^{\sim 3}$ [14]. This temperature dependence is not found in this theory. Indeed it is hard to see how such behaviour could arise in any theory involving a Fermi surface: any residual electron-electron scattering at the Fermi surface should at least give a T^2 resistivity which would dominate.

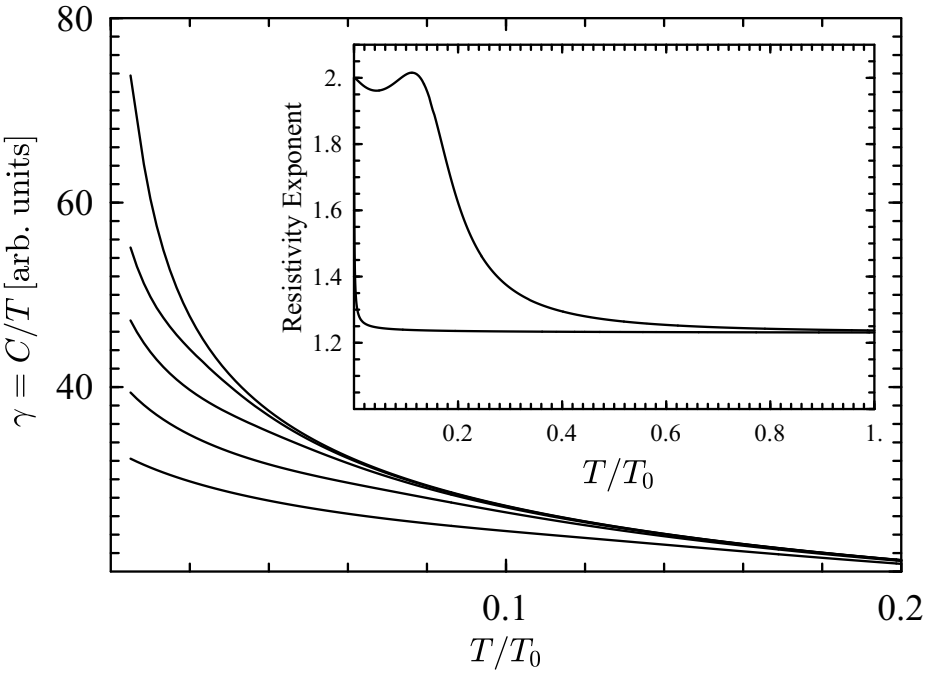

Fig. 6. Dependence of specific heat coefficient C/T on temperature T for $h = 0.01, .0.1, 0.2, 0.4$ calculated for a two dimensional metamagnetic critical point. Inset: Dependence of resistivity exponent $\partial \ln \rho / \partial \ln T$ on T for $h/H^* = 0$ (lower curve) and 0.1 (upper curve). (T_0 defined in text.)

The unusual resistivity at the critical point itself is very mysterious. It could perhaps be a consequence of a first order metamagnetic transition occurring at the lowest temperatures. The process whereby the higher magnetization phase nucleates in the lower magnetization one and the result of this on the resistivity is a possible avenue to be explored. A more speculative idea is that a novel metallic state has been found. Most metals at quantum critical points are unstable to other ordered phases. Either the transition goes first order (as is the case for MnSi) or superconductivity is induced. At the metamagnetic critical end-point neither of these states are possible: the magnetic field is too strong for superconductivity and we have deliberately tuned away the first order transition. Without the usual "escape routes" perhaps we are forcing the metamagnetic quantum critical metal to do something entirely different and new.

9 Conclusions

In conclusion, we have presented a theory of metamagnetic quantum criticality as it applies to the bilayer ruthenate $Sr_3Ru_2O_7$. We have obtained numerical solutions to the RG equations and used them to compute the differential susceptibility, the specific heat and the resistivity. Our theory accounts for the unusual

temperature dependence of $\chi(T, H = 0)$, the paramagnetic ground state and the main features of behaviour seen in $Sr_3Ru_2O_7$ as the metamagnetic critical point is approached. This lends weight to the assumptions underlying much of the recent work on quantum phase transitions and indeed on non-Fermi liquids. However, the puzzling behaviour of $Sr_3Ru_2O_7$ at the critical point itself [14] remains outside this framework. Subsequent papers [25] will present the most general case, and in particular apply the theory in three dimensional materials such as MnSi. We have shown already that the assumptions implicit in the conventional approach, which underlie much recent work on quantum phase transitions in metals and indeed on non-Fermi-liquid physics, are apparently consistent with much of the observed behaviour of $Sr_3Ru_2O_7$.

Acknowledgements: AJS acknowledges the support of the Royal Society and Leverhulme Trust. AJM was supported by NSF-DMR-0081075 and the EPSRC and thanks the Cavendish Laboratory, the Theoretical Physics group at the University of Birmingham and the Aspen Center for Physics for hospitality while parts of this work were undertaken. We thank A. P. Mackenzie for advice, encouragement and comments on the manuscript and D. J. Singh for helpful comments.

References

1. See, *e.g.* articles in *Proceedings of the 6th International Conference on Research in High Magnetic Fields*, published in *Physica*: B94-5, 2001 or in the SCES98 proceedings, *Physica*: B259-261, 1999.
2. H. Aoki, S. Uji, A. K. Albessard, and Y. Onuki. Transition of f electron nature from itinerant to localized: Metamagnetic transition in $CeRu_2Si_2$ studied via the de haas–van alphen effect. *Phys. Rev. Lett.*, 71(13):2110–2113, 1993.
3. D. Belitz, T. R. Kirkpatrick, A. J. Millis, and Thomas Vojta. Nonanalytic magnetization dependence of the magnon effective mass in itinerant quantum ferromagnets. *Phys. Rev. B*, 58(21):14155–14158, 1998.
4. D. Belitz, T. R. Kirkpatrick, and Thomas Vojta. Which quantum phase transitions are described by local order parameter field theories? cond-mat/0109547.
5. D. Belitz, T. R. Kirkpatrick, and Thomas Vojta. Nonanalytic behavior of the spin susceptibility in clean fermi systems. *Phys. Rev. B*, 55(15):9452–9462, 1997.
6. E. I. Blount. Symmetry properties of triplet superconductors. *Phys. Rev. B*, 32(5):2935–2944, 1985.
7. G. Busiello, L. De Cesare, and I. Rabuffo. Quenched-impurity influence on quantum critical behavior. *Phys. Rev. B*, 29(7):4189–4191, 1984.
8. L. Capogna, E. M. Forgan, S. M. Hayden, A. Wildes, J. A. Duffy, A. P. Mackenzie, R. S. Perry, S. Ikeda, Y. Maeno, and S. P. Brown. Observation of two-dimensional spin fluctuations in the bilayer ruthenate $Sr_3Ru_2O_7$ by inelastic neutron scattering. cond-mat/0201556.
9. S. Chakravarty, R. B. Laughlin, D. K. Morr, and C. Nayak. Hidden order in the cuprates. *Phys. Rev. B*, 63:094503, 2001.
10. Gennady Y. Chitov and Andrew J. Millis. Leading temperature corrections to fermi liquid theory in two dimensions. *Phys. Rev. Lett.*, 86(23):5337–5340, 2001.
11. P. Coleman, C. Pepin, Q. Si, and R. Ramazashvili. How do fermi liquids get heavy and die? *J. Phys.: Condens. Matter*, 13:R723–R738, 2001.

12. J. Flouquet, S. Kambe, L. P. Regnault, P. Haen, J. P. Brison, F. Lapierre, and P. Lajey. The heavy fermion compound $CeRu_2Si_2$ - magnetic instability, lattice quasicollapse and metamagnetism. *Physica*, B215(1):77–87, 1995.
13. P. Gegenwart, F. Kromer, M. Lang, G. Sparn, C. Geibel, and F. Steglich. Non-fermi-liquid effects at ambient pressure in a stoichiometric heavy-fermion compound with very low disorder: $CeNi_2Ge_2$. *Phys. Rev. Lett.*, 82(6):1293–1296, 1999.
14. S. A. Grigera, R. S. Perry, A. J. Schofield, M. Chiao, S. R. Julian, G. G. Lonzarich, S. I. Ikeda, Y. Maeno, A. J. Millis, and A. P. Mackenzie. Magnetic field-tuned quantum criticality in the metallic ruthenate $Sr_3Ru_2O_7$. *Science*, 294(5541):329–332, 2001.
15. P. Haen, J. Flouquet, F. Lapierre, P. Lejay, and G. Remenyi. Metamagnetic-like transition in $CeRu_2Si_2$. *J. Low Temp. Phys.*, 67(5-6):391–419, 1987.
16. T. Hamamoto, K. Kindo, T. C. Kobayashi, Y. Uwatoko, S. Araki, R. Settai, and Y. Onuki. Metamagnetic transition of $CeRh_2Si_2$ under high fields and high pressures at various temperatures. *Physica B*, 281-282:64–65, 2000.
17. John A. Hertz. Quantum critical phenomena. *Phys. Rev. B*, 14(3):1165–1184, 1976.
18. Shin-Ichi Ikeda, Yoshiteru Maeno, Masashi Kosaka, and Yoshiya Uwatoko. The ground state in $Sr_3Ru_2O_7$ revisited; fermi liquid close to a ferromagnetic instability. *Phys. Rev. B*, 62(10):R6089–R6092, 2000.
19. S R Julian, C Pfleiderer, F M Grosche, N D Mathur, G J McMullan, A J Diver, I R Walker, and G G Lonzarich. The normal states of magnetic d and f transition metals. *J. Phys.:condens. matt.*, 8(48):9675–9688, 1996.
20. A. P. Mackenzie, S. R. Julian, A. J. Diver, G. J. McMullan, M. P. Ray, G. G. Lonzarich, Y. Maeno, S. Nishizaki, and T. Fujita. Quantum oscillations in the layered perovskite superconductor Sr_2RuO_4. *Phys. Rev. Lett.*, 76(20):3786–3789, 1996.
21. Y. Maeno, H. Hashimoto, K. Yoshida, S. Nishizaki, T. Fujita, J. G. Bednorz, and F. Lichtenberg. Superconductivity in a layered perovskite without copper. *Nature*, 372(6506):532–534, 1994.
22. D. Meyer and W. Nolting. Strong-coupling scenario of a metamagnetic transition. *Phys. Rev. B*, 64:052404, 2001.
23. A. J. Millis. Effect of a nonzero temperature on quantum critical points in itinerant fermion systems. *Phys. Rev. B*, 48(10):7183–7195, 1993.
24. A. J. Millis, A. J. Schofield, G. G. Lonzarich, and S. A. Grigera. Metamagnetic quantum criticality in metals. cond-mat/0109440. To appear in *Phys. Rev. Lett.*, 2002.
25. A. J. Millis, A. J. Schofield, G. G. Lonzarich, and S. A. Grigera. Theory of metamagnetic quantum criticality in metals. *To be published.*
26. John W. Negele and Henri Orland. *Quantum many-particle systems.* Addison-Wesley Publishing Company, Inc., 1987.
27. R. S. Perry, L. M. Galvin, S. A. Grigera, L. Capogna, A. J. Schofield, A. P. Mackenzie, M. Chiao, S. R. Julian, S. I. Ikeda, S. Nakatsuji, Y. Maeno, and C. Pfleiderer. Metamagnetism and critical fluctuations in high quality single crystals of the bilayer ruthenate $Sr_3Ru_2O_7$. *Phys. Rev. Lett.*, 86(12):2661–2664, 2001.
28. T. M. Rice. Superconductivity: An analogue of superfluid ^{3}He. *Nature*, 396:627–629, 1998.
29. A. Rosch. Interplay of disorder and spin fluctuations in the resistivity near a quantum critical point. *Phys. Rev. Lett.*, 82(21):4280–4283, 1999.
30. Hiroyuki Satoh and Fusayoshi J. Ohkawa. Theory of the metamagnetic crossover in $CeRu_2Si_2$. *Phys. Rev. B*, 63:184401, 2001.

31. A. Schröder, G. Aeppli, R. Coldea, M. Adams, O. Stockert, H. v. Löhneysen, E. Bucher, R. Ramazashvili, and P. Coleman. Onset of antiferromagnetism in heavy-fermion metals. *Nature*, 407(6802):351–355, 2000.
32. D. J. Singh and I. I. Mazin. Electronic structure and fermiology of $Sr_3Ru_2O_7$. *Phys. Rev. B*, 63:165101, 2001.
33. Edmund C. Stoner. Ferromagnetism. *Rep. Prog. Phys.*, 11:43–112, 1947.
34. M. B. Suvasini, G. Y. Guo, W. M. Temmerman, and G. A. Gehring. Metamagnetic transition and magnetic properties of UPt_3. *Phys. Rev. Lett.*, 71(18):2983–2986, 1993.
35. C Thessieu, C Pfleiderer, A N Stepanov, and J Flouquet. Field dependence of the magnetic quantum phase transition in MnSi. *J. Phys.:condens. matt.*, 9(31):6677–6687, 1997.
36. Hilbert von Löhneysen. Non-fermi-liquid behaviour in the heavy-fermion system $CeCu_{6-x}Au_x$. *J. Phys.:condens. matt.*, 8(48):9689–9706, 1996.
37. H. Yamada. Metamagnetic transition and susceptibility maximum in an itinerant-electron system. *Phys. Rev. B*, 47(17):11211–11219, 1993.
38. H. Yamada and K. Terao. Itinerant-electron metamagnetism of MnSi at high pressure. *Phys. Rev. B*, 59(14):9342–9347, 1999.